



1 The importance of spatio-temporal snowmelt variability for 2 isotopic hydrograph separation in a high-elevation catchment

3 Jan Schmieder¹, Florian Hanzer¹, Thomas Marke¹, Jakob Garvelmann², Michael Warscher²,
4 Harald Kunstmann² and Ulrich Strasser¹

5 ¹Institute of Geography, University of Innsbruck, Innsbruck, 6020, Austria

6 ²Institute of Meteorology and Climate Research - Atmospheric Environmental Research, Karlsruhe Institute of
7 Technology, Garmisch-Partenkirchen, 82467, Germany

8 *Correspondence to:* Jan Schmieder (Jan.Schmieder@uibk.ac.at)

9 **Abstract.** Seasonal snow cover is an important temporary water storage in high-elevation regions. Especially in
10 remote areas, the available data is often insufficient to explicitly quantify snowmelt contributions to streamflow.
11 The unknown spatio-temporal variability of the snowmelt isotopic content, as well as pronounced spatial
12 variations of snowmelt rates lead to high uncertainties in applying the isotopic hydrograph separation method.
13 This study presents an approach that uses a distributed snowmelt model to support the traditional isotopic
14 hydrograph separation technique. The stable isotopic signatures of snowmelt water samples collected during two
15 spring 2014 snowmelt events at a north- and a south-facing slope were volume-weighted with snowmelt rates
16 derived from a distributed physics-based snow model in order to transfer the measured plot-scale isotopic
17 content of snowmelt water to the catchment scale. The observed $\delta^{18}\text{O}$ values and modelled snowmelt rates
18 showed distinct inter- and intra-event variations, as well as marked differences between north- and south-facing
19 slopes. Accounting for those differences, two-component isotopic hydrograph separation revealed snowmelt
20 contributions of $35\pm 3\%$ and $75\pm 14\%$ for the early and peak melt season, respectively. Differences to formerly
21 used weighting methods (e.g. using observed plot-scale melt rates) or considering either the north- or south-
22 facing slope were up to 5 and 15 %, respectively.

23 1 Introduction

24 The seasonal snow cover is an important temporary water storage in alpine regions. For water resources
25 management, the timing and amount of water released from this storage is important to know, especially in
26 downstream regions where the water is needed (drinking water, snow making, hydropower, irrigation water) or
27 where it represents a potential risk (flood, drought). In many headwater catchments, seasonal water availability is
28 strongly dependent on cryospheric processes and understanding these processes becomes even more relevant in a
29 changing climate (APCC, 2014; IPCC, 2013; Weingartner and Aschwanden, 1992). Environmental tracers are a
30 tool to investigate the relevant processes, but scientific studies are still rare for high-elevation regions because of
31 the restricted access and high risk for field measurements in these challenging conditions.

32 Two-component isotopic hydrograph separation (IHS) is a technique to separate streamflow into different time
33 source components (event water, pre-event water) (Sklash et al., 1976). The event component depicts water that
34 enters the catchment during an event (e.g. snowmelt) and is characterized by a distinct isotopic signature,
35 whereas pre-event water is stored in the catchment prior to the onset of the event and is characterized by a
36 different isotopic signature (Sklash and Farvolden, 1979; Sklash et al., 1976). The technique dates back to the
37 late 1960s (Pinder and Jones, 1969) and was initially used for separating storm hydrographs in humid



1 catchments. The first snowmelt-based studies were conducted in the 1970s by Dincer et al. (1970) and Martinec
2 et al. (1974). These studies showed a large pre-event water fraction (>50 %) of streamflow and changed the
3 understanding of the processes in catchment hydrology fundamentally (Klaus and McDonnell, 2013; Sklash and
4 Farvolden, 1979) and forced a paradigm shift, especially for humid temperate catchments. However, other
5 snowmelt-based studies (Huth et al., 2004; Liu et al., 2004; Williams et al., 2009) reveal a large contribution of
6 event water (>70 %), i.e. in permafrost or high-elevation catchments, depending on the system state (e.g. frost
7 layer thickness and snow depth), catchment characteristics and runoff generation mechanisms.

8 Klaus and McDonnell (2013) highlighted the need for accounting and quantifying the spatial variability of the
9 isotope signal of event water, which is still a vast uncertainty in snowmelt-based IHS. In the literature
10 inconclusive results prevail with respect to the variation of the snowmelt isotopic signal. Spatial variability of
11 snowmelt isotopic composition was statistically significant related to elevation (Beaulieu et al., 2012) in a
12 catchment in British Columbia, Canada with 500 m relief. Moore (1989) and Laudon et al. (2007) found no
13 statistical significant variation in their snowmelt $\delta^{18}\text{O}$ data, due to the low gradient and small elevation range
14 (approximately 30 m and 290 m) in their catchments which favours an isotopically more homogenous snow
15 cover. The effect of the aspect of the hillslopes on isotopic variability and IHS results in topographically
16 complex terrain has also been rarely investigated. Dahlke and Lyon (2013) and Dietermann and Weiler (2013)
17 surveyed the snowpack isotopic content and showed a notable spatial variability in their data, particularly
18 between north- and south-facing slopes. They conclude that the spatial variability of snowmelt could be high and
19 that the timing of meltwater varies with the morphology of the catchment. Dietermann and Weiler (2013) also
20 concluded that an elevation effect (decrease of snowpack isotopic signature with elevation), if observed, is
21 disturbed by fractionation due to melt/refreeze processes during the ablation period. These effects most likely
22 superimpose the altitudinal gradient. Aspect and slope are therefore important factors that control the isotopic
23 evolution of the snow cover and its melt (Cooper, 2006). In contrast, there have been various studies that have
24 investigated the temporal variability of the snowmelt isotopic signal, e.g. by the use of snow lysimeters (Hooper
25 and Shoemaker, 1986; Laudon et al., 2002; Liu et al., 2004; Maulé and Stein, 1990; Moore, 1989; Williams et
26 al., 2009). During the ablation season the isotopic evolution of the snowpack progresses due to percolating rain
27 water and fractionation caused by melting, refreezing and sublimation (Dietermann and Weiler, 2013; Lee et al.,
28 2010; Unnikrishna et al., 2002; Zhou et al., 2008), which leads to a homogenization of the isotopic profile of the
29 snowpack (Árnason et al., 1973; Dinçer et al., 1970; Stichler, 1987) and an increase in heavy isotopes of
30 meltwater throughout the freshet period (Laudon et al., 2007; Taylor et al., 2001; Taylor et al., 2002;
31 Unnikrishna et al., 2002). Therefore the characterization and the use of the evolving isotopic signal of snowmelt
32 water instead of single snow cores is crucial for applying IHS (Taylor et al., 2001; 2002).

33 There have been various approaches to cope with the variability of the input signal. If one uses more than one
34 $\delta^{18}\text{O}$ snowmelt value for applying the IHS method, it is important to weight the values with appropriate melt
35 rates, e.g. measured from the outflow of a snow lysimeter. Common weighting methods are the volume-
36 weighted average approach (VWA), as used by Mast et al. (1995) and the current meltwater approach (CMW),
37 applied by Hooper and Shoemaker (1986). Laudon et al. (2002) developed the runoff-corrected event water
38 approach (runCE), which accounts for both, the temporal isotopic evolution and temporary storage of meltwater
39 in the catchment and overcomes the shortcomings introduced by VWA and CMW. This method was furthermore
40 deployed in several snowmelt-based IHS (Beaulieu et al., 2012; Carey and Quinton, 2004; Laudon et al., 2004;
41 Laudon et al., 2007).



1 Tracers have successfully been used in modelling studies to provide empirical insights into runoff generation
2 processes and catchment functioning (Birkel and Soulsby, 2015; Birkel et al., 2011; Capell et al., 2012;
3 Uhlenbrook and Leibundgut, 2002), but the combined use of distributed modelling and isotopic tracers in snow-
4 dominated environments is rare. Ahluwalia et al. (2013) used an isotope and a modelling approach to derive
5 snowmelt contributions to streamflow and determined differences between the two techniques of 2 %.
6 Distributed modelling can provide areal melt rates that can be used for weighting the measured isotopic content
7 of meltwater. Pomeroy et al. (2003) describe the differences of insolation between north- and south-facing slopes
8 in complex terrain that lead to spatial varying melt rates of the snowpack throughout the freshet period. The use
9 of the areal snowmelt data from models will likely reduce the uncertainty that arises from the representativeness
10 of measured melt rates at the plot-scale.

11 The overall goal of our study was to quantify the streamflow contribution from snowmelt and hence to improve
12 the knowledge of hydroclimatological processes in high-elevation catchments. This study aims to test a
13 technique that could enhance the reliability of isotopic hydrograph separation, and thus the estimation of
14 snowmelt contributions to streamflow by considering the distinct spatio-temporal variability of snowmelt and its
15 isotopic signature in a high-elevation study region. This study has the following three objectives: 1) the
16 estimation of the spatio-temporal variability of snowmelt and its isotopic content, 2) the quantification of its
17 impact on isotopic hydrograph separation (IHS) and 3) to combine a physically-based snowmelt model with
18 traditional IHS. Distributed melt rates provided by a surface energy balance model were used to weight the
19 measured isotopic content of snowmelt in order to characterize the event water isotopic content. Traditional
20 weighting methods (e.g. using plot-scale observed melt rates) are compared with the newly proposed approach.
21 This study provides an integrated approach for streamflow components evaluation based on experimental field
22 work (data collection) and modelling as requested in previous studies (e.g. Seibert and McDonnell, 2002).

23 **2 Study area**

24 The 98 km² high-elevation catchment of the stream Rofenache is located in the Central Eastern Alps (Oetztal
25 Alps, Austria), close to the main Alpine ridge. The study area has a dry inner-alpine climate. Mean annual
26 precipitation is 800 mm yr⁻¹, of which 44 % falls as snow. The mean annual temperature at the gauging station in
27 Vent (1890 m.a.s.l., reference period: 1982-2003) is 2°C. Seasonal snow cover typically lasts from October to
28 the end of June at the highest regions of the valley. The basin ranges in elevation from approximately 1900
29 m.a.s.l. to 3770 m.a.s.l. Average slope is 25° and average elevation is 2930 m.a.s.l. (calculated from a 50 m
30 digital elevation model). A thin riparian zone (<100 m width) is located in the valley floor. The predominantly
31 south- and north-facing slopes form the main valley, which trends roughly from west to east (cf. Fig. 1).

32 The bedrock consists of mainly paragneiss and mica schist and is overlain by a mantle of glacial deposit and thin
33 soils (< 1 m). The bedrock outcrops and unconsolidated bare rocks cover the largest part (42 %) of the catchment
34 (CLC, 2006). Glaciers cover approximately a third of the Rofen valley area (35 %), while pastures and
35 coniferous forests are located in the lowest parts of the catchment and cover less than 0.5 % (CLC, 2006).
36 Sparsely vegetated areas and natural grassland cover 15 and 7.5 %, respectively (CLC, 2006). Besides seasonally
37 frozen ground at slopes on various expositions, permafrost is likely to occur at an altitude over 2600 m.a.s.l. at
38 the north-facing slopes (Haerberli, 1975). The annual hydrograph reveals a highly seasonal flow regime. The
39 mean annual discharge is 4.5 m³ s⁻¹ (reference period: 1971-2009) and is dominated by snow and glacier melt



1 during the ablation season, which typically lasts from May to September. The onset of the early snowmelt season
2 in the lower part of the basin is typically in April.

3 **3 Methods**

4 **3.1 Field sampling, measurements and laboratory analysis**

5 The field work was conducted during the 2014 snowmelt season between the beginning of April and the end of
6 June. Two short-term melt events (3 days) were investigated to illustrate the difference between early spring
7 season melt and peak melt. Low discharge and air temperatures with a small diurnal variation and low melt rates,
8 as well as a snow-covered area (SCA) of about 90 % in the basin (Fig. 7a) are the boundary conditions of the
9 early melt event at the end of April (cf. Fig. 2b). In contrast, the peak melt period at the end of June is
10 characterized by high discharge and melt rates, a flashy hydrograph, high air temperatures with remarkable
11 diurnal variations (Fig. 2c) and a strongly retreated snowline (SCA: 66 %; cf. Fig. 7c). Both events followed dry
12 antecedent conditions (no observed precipitation for at least 2 days) and no precipitation during the events itself
13 (Fig. 2). Discharge data are available at an hourly resolution for the gauging station in Vent and meteorological
14 data are obtained by 20 automatic weather stations (hourly resolution) located in and around the basin (Fig. 1).

15 The stream water sampling for stable isotope analysis consists of pre-freshet baseflow samples at the beginning
16 of March, sub-daily grab samples during the two studied events and a post-event sample in July as indicated in
17 Fig. 2a (grey-shaded area). Snowmelt, snowpack and surface overland flow (if observed) samples were collected
18 at the south- (S1, S2) and north-facing slope (N1, N2), as well as on a wind-exposed ridge shown in Fig. 1 using
19 a snowmelt collector. At each test site a snow pit was dug to install a 0.1 m² polyethylene snowmelt collector at
20 the ground-snowpack interface. The snowmelt collector consists of a pipe that drains the percolating meltwater
21 into a fixed plastic bag. Tests yield a preclusion of evaporation for this sampling method. Composite daily
22 snowmelt water samples (bulk sample) were collected in these bags and transferred to polyethylene bottles in the
23 field before the onset of the diurnal melt cycle. Furthermore sub-daily grab melt samples were collected to define
24 the diurnal variability. The pit face was covered with white styrofoam to protect it from direct sunlight. Stream,
25 surface overland flow and grab snowmelt water samples were collected in 20 mL polyethylene bottles. Snow
26 samples from snow pit layers were filled in airtight plastic bags and melted below room temperature before
27 refilling them in bottles. Overall, 144 samples were taken during the study period. Snow water equivalent
28 (SWE), snow height (HS), snow density (SD), and various snowpack observations (wetness and hand hardness
29 index) were observed before the onset of the diurnal melt cycle at the study plots (Fig. 1). Mean SWE was
30 determined by averaging five snow tube measurements within an area of 20 m² at each site. Daily melt rates
31 were calculated by subtracting succeeding SWE values. Sublimation was neglected, as it contributes only to a
32 small percentage (~10 %) to the seasonal water balance in high altitude catchments in the Alps (Strasser et al.,
33 2008).

34 All samples were treated by the guidelines as proposed by Clark and Fritz (1997) and were stored dark and cold
35 until analysis. The $\delta^{18}\text{O}$ and δD content was measured with cavity ring-down spectroscopy (Picarro L1102-i).
36 The mean laboratory precision (replication of 8 measurements) for all measured samples was 0.06 ‰ for $\delta^{18}\text{O}$.
37 Due to the covariance of $\delta^2\text{H}$ (δD) and $\delta^{18}\text{O}$ (Fig. 3) all analyses were made with oxygen-18 values. Results are
38 expressed in the delta notation as parts per thousand relative to the Vienna Standard Mean Ocean Water
39 (VSMOW2).



1 3.2 Model description

2 For the simulation of the daily melt rates, the non-calibrated, distributed, and physically-based
 3 hydroclimatological model AMUNDSEN (Strasser, 2008) was applied. Model features include interpolation of
 4 meteorological fields from point measurements (Marke, 2008; Strasser, 2008); simulation of short- and
 5 longwave radiation, including topographic and cloud effects (Corripio, 2003; Greuell et al., 1997);
 6 parameterization of snow albedo depending on snow age and temperature (Rohrer, 1992); modelling of forest
 7 snow and meteorological processes (Liston and Elder, 2006; Strasser et al., 2011); lateral redistribution of snow
 8 due to gravitational (Gruber, 2007) and wind-induced (Helfricht, 2014; Warscher et al., 2013) processes; and
 9 determination of snowmelt using an energy balance approach (Strasser, 2008). Besides having been applied for
 10 various other Alpine sites in the past (Hanzer et al., 2014; Marke et al., 2015; Pellicciotti et al., 2005; Strasser,
 11 2008; Strasser et al., 2008; Strasser et al., 2004), AMUNDSEN has recently been set up and extensively
 12 validated for the Oetztal Alps region (Hanzer et al., 2016). This setup was also used to run the model in the
 13 presented study for the period 2013–2014 using a temporal resolution of 1 hour and a spatial resolution of 50
 14 meters. In order to determine the model performance during the study period, catchment-scale snow distribution
 15 by satellite-derived binary snow cover maps and plot-scale observed SWE data were used for the validation.
 16 Therefore the spatial snow distribution as simulated by AMUNDSEN was compared with a set of MODIS (500
 17 m spatial resolution) and Landsat (30 m resolution, subsequently resampled to the 50 m model resolution) snow
 18 maps with less than 10 % cloud coverage over the study area using the methodology described in Hanzer et al.
 19 (2016). Model results were evaluated using the performance measures BIAS, accuracy (ACC) and critical
 20 success index (CSI) (Zappa, 2008). ACC represents the fraction of correctly classified pixels (either snow-
 21 covered or snow-free both in the observation and the simulation). CSI describes the number of correctly
 22 predicted snow-covered pixels divided by the number of times where snow is predicted in the model and/or
 23 observed, and BIAS corresponds to the number of snow-covered pixels in the simulation divided by the
 24 respective number in the observation. ACC and CSI values range from 0 to 1 (where 1 is a perfect match), while
 25 for BIAS values below 1 indicate underestimations of the simulated snow cover, and values above 1 indicate
 26 overestimations. At the plot-scale, observed SWE values were compared with AMUNDSEN SWE values
 27 represented by the underlying pixel at the location of the snow course. Catchment-scale melt rates are calculated
 28 by subtracting two consecutive daily SWE grids, not considering sublimation to be comparable to the plot-scale
 29 observed melt rates. Subsequently, the DEM was used to calculate an aspect grid and further to divide the
 30 catchment into two parts: grid cells with aspects ranging from $\geq 270^\circ$ to $\leq 90^\circ$ were classified as ‘north-facing’,
 31 while the remaining cells were attributed to the class ‘south-facing’. Finally these two grids were combined to
 32 derive melt rates for the south-facing ($melt_s$) and for the north-facing slope ($melt_n$).

33 3.3 Isotopic hydrograph separation, weighting approaches and uncertainty analysis

34 IHS is a steady-state tracer mass balance approach and several assumptions underlie this simple principle, which
 35 are described and reviewed in Buttle (1994) and Klaus and McDonnell (2013). The focus of this study relies on
 36 one of those assumptions: the spatio-temporal variability of event water isotopic signature is absent or can be
 37 accounted for. The fraction of event water (f_e) contributing to streamflow was calculated from Eq. (1).

$$38 \quad f_e = \frac{(C_p - C_s)}{(C_p - C_e)} \quad (1)$$



1 The tracer concentration of the pre-event component (C_p) is the $\delta^{18}\text{O}$ content of baseflow prior to the onset of the
2 freshet period, constituted mainly by groundwater and eventually by soil water which was assumed to have the
3 same isotopic signal. Tracer concentration C_s is the isotopic content of stream water samples for each sampling
4 time. The isotopic compositions of snowmelt samples were weighted differently to compose the event water
5 tracer concentration (C_e). Therefore the following five weighting approaches were deployed in the analyses:

- 6 (1) volume-weighted with observed plot-scale melt rates (VVO)
- 7 (2) equally weighted, assuming an equal melt rate on north- and south-facing slopes (VWE)
- 8 (3) no weighting, only south-facing slopes considered (SOUTH)
- 9 (4) no weighting, only north-facing slopes considered (NORTH)
- 10 (5) volume-weighted with simulated catchment-scale melt rates (VWS)

11 Equation (2) is the VWS approach with simulated melt rates for north- and south-facing slopes as described in
12 Section 3.2, where M is the simulated melt rate (in mm), $\delta^{18}\text{O}$ is the isotopic content of sampled snowmelt and
13 subscripts s and n indicate north and south, respectively. For depicting C_e a daily timestep (t) is used,
14 considering daily melt rates and daily bulk snowmelt isotopic content.

$$15 \quad C_e(t) = \frac{M_s(t)\delta^{18}\text{O}_s(t) + M_n(t)\delta^{18}\text{O}_n(t)}{M_s(t) + M_n(t)} \quad (2)$$

16 An uncertainty analysis (Eq. (3)) was performed according to the Gaussian standard error method proposed by
17 Genereux (1998):

$$18 \quad W_{f_e} = \left\{ \left[\frac{C_p - C_s}{(C_p - C_e)^2} W_{C_e} \right]^2 + \left[\frac{C_s - C_e}{(C_p - C_e)^2} W_{C_p} \right]^2 + \left[\frac{-1}{(C_p - C_e)^2} W_{C_s} \right]^2 \right\}^{1/2}, \quad (3)$$

19 where W is the uncertainty, C is the isotopic content, f is the fraction and the subscripts p, s and e refer to the
20 pre-event, stream and event component. The assumption of negligible errors in the discharge measurement and
21 the melt rates (modelled and observed) underlay this method. The uncertainty of streamflow (W_{C_s}) is assumed to
22 be equal to the laboratory precision (0.06 ‰). For the uncertainty of the event component (W_{C_e}), the diurnal
23 temporal variation of the snowmelt isotopic signal was used (0.5 ‰) and an error of 0.04 ‰ was assumed for the
24 pre-event component (W_{C_p}), which reflects the standard deviation of the two baseflow samples. IHS results
25 correspond to the 95 % confidence level. Spatial variations were not considered in this error calculation method
26 as they represent the hydrologic signal of interest.

27 4 Results

28 4.1. Spatio-temporal variability of stable isotopic signature of sampled of water sources

29 The quality control was performed by the $\delta^2\text{H}-\delta^{18}\text{O}$ plot (Fig. 3) which indicates that no shift of the linear
30 regression line due to secondary fractionation effects (evaporation) during storage and transport of the samples
31 occurred. The slope of the linear regression (slope=8.5, $n=144$, $R^2=0.93$) of the measurement data slightly
32 deviates from that of the global meteoric (slope=8) and local meteoric water line (slope=8.1) delineated by
33 monthly data from the ANIP (Austrian Network of Isotopes in Precipitation) sampling site in Obergurgl, which
34 is located in an adjacent valley (reference period: 1991-2014). The small deviation (visible in Fig. 3) of the
35 sampled water sources (i.e. snowpack and snowmelt) could indicate fractionation effects induced by phase



1 transition (i.e. melt/refreeze and sublimation). The significant differences between isotopic signatures of pre-
2 event streamflow and snowmelt water enabled the IHS.
3 Overall, the $\delta^{18}\text{O}$ values ranged from -21.5 to -15 ‰, while snowpack samples are characterized by the most
4 negative and pre-event baseflow samples by the least negative values. Snowpack samples show a wide isotopic
5 range, while streamflow samples reveal the narrowest spread, reflect a composite isotopic signal and indicate
6 mixing processes of the water components. Figure 4 shows the $\delta^{18}\text{O}$ data of the water samples grouped into
7 different categories and split into early and peak melt data. It shows the different $\delta^{18}\text{O}$ ranges and medians of the
8 sampled water sources (Fig. 4a), as well as marked spatio-temporal variations of the isotopic signal (Fig. 4b and
9 c). It is apparent that the snowpack $\delta^{18}\text{O}$ values have a larger variation compared to the snowmelt data due to
10 homogenization effects (Fig. 4a), as was also shown by Árnason et al. (1973), Dincer et al. (1970) and Stichler
11 (1987). In contrast, the median of the $\delta^{18}\text{O}$ content of snowmelt was higher than that of the snowpack, implicit in
12 the fractionation processes. The median of surface overland flow $\delta^{18}\text{O}$ was higher than that of snowmelt (Fig. 4a)
13 for the early and peak melt period. Overall, the $\delta^{18}\text{O}$ peak melt values (Fig. 4b) reveal less variation and a higher
14 median than the early melt values, because fractionation effects (due to melt/refreeze and sublimation) most
15 likely altered the isotopic content over time (cf. Taylor et al., 2001, 2002). One major finding was that the north-
16 facing slope $\delta^{18}\text{O}$ data reveals a larger range and a lower median compared to the opposing slope (Fig. 4c).
17 Samples from the wind drift influenced site (also south-exposed) were more depleted in heavy isotopes
18 compared to the south-facing slope samples (Fig. 4c).
19 In general, the average snowmelt and snowpack isotopic content was more depleted for the early melt period
20 (Table 1) and changed over time because fractionation was likely to alter the snowpack and its melt. It is obvious
21 that the isotopic evolution (gradually enrichment) on the south-facing slope took place earlier in the annual
22 melting cycle of snow, following a less marked isotopic change between early and peak melt and indicates a
23 premature snowpack concerning the enrichment of isotopes and early ripening compared to the north-facing
24 slope.
25 Table 1 shows that meltwater sampling throughout the entire snowmelt period is required to account for the
26 temporal variation (cf. Taylor et al., 2001, 2002). In detail, the snowpack and snowmelt $\delta^{18}\text{O}$ data highlighted a
27 marked spatial inhomogeneity between north- and south-facing slopes throughout the study period. The
28 snowpack isotopic composition from both sampled slopes was statistically different for the early melt, but not
29 for the peak melt (with Kruskal-Wallis test at 0.05 significance level), whereas the snowmelt $\delta^{18}\text{O}$ showed a
30 significant difference throughout the complete study period (Fig. 5).
31 Stream water isotopic content was more enriched in heavy isotopes during the early melt period and successively
32 became more depleted throughout the freshet period resulting in more negative values during peak melt (Table
33 2). The standard deviation and range of stream water $\delta^{18}\text{O}$ during early melt was higher and could be related to a
34 more increasing snowmelt contribution throughout the event and larger diurnal amplitudes of snowmelt
35 contribution compared to peak melt (Table 2, Fig. 11).

36 4.2 Snow model validation and snowmelt variability

37 Figure 6 shows the values for the selected performance measures based on the available MODIS and Landsat
38 scenes during the period March–July 2014, while Fig. 7 shows the observed and simulated spatial snow
39 distribution around the time of the two events. The results indicate a reasonable model performance with a



1 tendency to slightly overestimate the snow cover during the peak melt season (BIAS >1). In general the CSI
2 does not drop below 0.7 and 80 % of the pixels are correctly classified (ACC) throughout the study period.
3 Table 3 holds the observed and simulated SWE values at the plot-scale. The model slightly underestimates SWE
4 during peak melt, but generally appears to be in quite good agreement, suggesting well simulated snowpack
5 processes. Throughout the study period the model deviates by 13 % from the observed SWE values, but the
6 representativeness (small-scale effects) of SWE values represented by the respective 50 m pixel should be
7 considered.
8 Snowmelt (observed and simulated inter-daily losses of SWE) showed a distinct spatial variation between the
9 north-facing and the south-facing slope for the early melt (23/24 April), but less marked variations for the peak
10 melt (07/08 June) (Fig. 8). Relative day-to-day differences are more pronounced for the early melt season. Both
11 simulated and observed melt rates are higher for the peak melt event on the south-facing slope, but not for the
12 north-facing slope. Simulated melt intensity on the south-facing slope at the end of April was twice the rate on
13 the north-facing slope, while melt rates were approximately the same for the opposing slopes during peak melt.
14 Small-scale snowmelt variability during early melt (north-facing slope) and partly during peak melt (south-
15 facing slope on 07 June) probably due to micro-topographic effects caused contrasting results between simulated
16 and observed melt rates (Fig. 8).

17 **4.3 Weighting techniques and isotopic hydrograph separation**

18 Differences between the applied weighting techniques, induced by the high spatial variability of snowmelt
19 (Section 4.2), led to different event water isotopic compositions (C_e) used in the IHS analyses. Table 4 lists the
20 event water isotopic content (C_e) for the five deployed weighting approaches (cf. Section 3.3). The event water
21 component is depleted in $\delta^{18}\text{O}$ by roughly 0.3 ‰ for the second day (24 April) of the early melt event compared
22 to the preceding day, but inter-daily variation during the peak melt is almost absent. Especially during early melt
23 (23/04 to 24/04) strong deviations between observed plot-scale melt rates and distributed (areal) melt rates
24 obtained by AMUNDSEN occurred (Fig. 9), and led to more differing event water isotopic compositions
25 between the VWS and the VWO approach (Table 4).

26 IHS provides estimated contributions of event and pre-event water. The event water component is labelled as the
27 weighted snowmelt end-member. The hydrograph and the results of the IHS applied with the VWS method for
28 the early and peak melt event are presented in Fig. 10. Lower flow rates and higher pre-event fractions during
29 early melt (Fig. 10c) and vice versa for the peak melt period (Fig. 10d) are identifiable. The total runoff volume
30 during the peak melt period was approximately six times higher than in the early melt period. The fraction of
31 snowmelt (volume) estimated with the VWS approach was 35 and 75 % with calculated uncertainties (95 %
32 significance level) of 3 and 14 % for the early and peak melt event, respectively. Throughout the early melt
33 event, the snowmelt fraction increased from 25 to 44 % (Fig. 10c; Table 5). This trend mirrors the stream
34 isotopic content, which is descending (Fig. 10a). Event water contribution during peak melt was generally higher
35 but revealed a lower range (70 to 78 %; Fig. 10d). Diurnal isotopic variations of stream water are weak for both
36 events (Fig. 10a and b), and could not clearly be obtained due to missing data at the falling limbs of the
37 hydrographs.

38 The uncertainty calculated from Eq. (3) of the IHS applied with the VWS method in the present study was higher
39 (14 %) for the peak melt event because the difference between isotopic content of pre-event water and event



1 water was less than for the first event (3 %) (cf. Table 2 and 4). This difference controls the uncertainty the most
2 (cf. Section 3.3).

3 The use of five different weighting approaches led to strongly varying estimated snowmelt fractions of
4 streamflow (Fig. 11). Especially the differences between the SOUTH and the NORTH approach during both
5 investigated events (up to 24 %), and the differences between the VWS and the VWO approach (5 %) during
6 early melt (Fig. 11a) are notable. Event water contributions estimated by the different weighting methods (cf.
7 Section 3.3) range from 21-28 % at the beginning of the early melt event up to 31-55 % at the end of the event
8 (cf. Fig. 11a, Table 6). Minimum event water contributions during peak melt were estimated with 60-84 % and
9 maxima ranged between 67-94 % for the different weighting methods (Table 6, Fig. 11b). Beside these intra-
10 event variations in snowmelt contribution, the volumetric variations at the event-scale were smaller and ranged
11 between 28 to 40 % and 66 to 90 %, for the early and peak melt event, respectively (Table 6).

12 Considering only spatial variations of snowmelt isotopic signatures (i.e. comparing the NORTH/SOUTH
13 approach with the VWE approach) for IHS lead to differences in estimated event water fractions of maximum 7
14 and 14 % for the early and peak melt period, respectively (Table 6). However, considering only spatial variations
15 of snowmelt rates (i.e. comparing the VWS/VWO approach with the VWE approach) lead to maximum
16 differences in event water fraction of 3 and 2 % for the early and peak melt period, respectively (Table 6).

17 Surface overland flow was not considered in the IHS analyses because it reflects a runoff generation process
18 (geographic source) and hence is not a time source component of streamflow. However, if applied, it would most
19 likely increase the calculated snowmelt fraction slightly. Furthermore, snowmelt samples from the wind-exposed
20 site were not used in the IHS analyses because this site was only sampled on the south-facing slope during early
21 melt and is hardly representative for the catchment due to its limited coverage. However, an incorporation of this
22 data would decrease the calculated snowmelt fraction by approximately 2 %.

23 **5 Discussion**

24 **5.1 Variations of streamflow**

25 Snowmelt is a major contributor to the hydrograph during the spring freshet period in alpine regions and
26 remarkable amounts of snowmelt water infiltrate into the soil and recharge groundwater (Penna et al., 2014).
27 During the whole study period, two major snowmelt pulses (Mid-May and beginning of June) followed four less
28 pronounced ones during mid-March to early May (Fig. 2a). The hydrological response followed the variations of
29 air temperature, as already observed by Braithwaite and Olesen (1989), because the available net-shortwave
30 energy mostly controls the magnitude of snowmelt (Hock, 2003) (Fig. 2a). Peak melt occurred at the beginning
31 of June with maximum daily temperatures and runoff, of 15 °C and 18 mm d⁻¹, respectively. The following high-
32 flows were affected by rain (Fig. 2a) and by glacier melt due to the strongly retreated snow line and snow-free
33 ablation area of the glaciers in July. Diurnal variations in discharge were strongly correlated with diurnal
34 variations of air temperature (Fig. 2a and b) with a time lag of 3-5 hours for the early melt event and 2-3 hours
35 for the peak melt event. These time lags are common in mountain catchments (Engel et al., 2015; Schuler, 2002).
36 During peak melt, the flashy hydrograph revealed less variation in the timing of peak discharge of 7 day data
37 (cf. Fig. 2c) compared to the early melt, as well reported by Lundquist and Cayan (2002). An inverse
38 relationship between streamflow δ¹⁸O and discharge (and thus snowmelt contribution) was found for the early
39 melt event (Fig. 10a and c). Diurnal responses of streamflow δ¹⁸O were slightly identified for both events, but



1 masked due to missing data during the recession of the hydrograph. These results confirm earlier findings of
2 Engel et al. (2015) who identified inverse relationships between streamflow $\delta^{18}\text{O}$ and discharge during several
3 24-hour events in an adjacent valley on the southern side of the main Alpine ridge, although their findings rely
4 on streamflow contributions from snow as well as glacier melt. The lower stream water isotopic content during
5 peak melt suggests a remarkable contribution of more depleted snowmelt to streamflow and therefore confirms
6 the results of the IHS (Section 5.4).

7 **5.2 Spatio-temporal variability of snowmelt and its isotopic signature**

8 The magnitude of snowmelt varies in catchments with complex topography (Carey and Quinton, 2004; Dahlke
9 and Lyon, 2013; Pomeroy et al., 2003). This was also demonstrated for the Rofen valley in the presented study
10 (Fig. 8, Table 3). The small-scale snowmelt variability was high, as plot-scale observed melt rates contradicted
11 distributed melt rates during early melt (Fig. 9), a period of the snowmelt season when snow cover processes are
12 typically very heterogeneous across the catchment. The peak melt period was characterised by less spatial and
13 day-to-day variation in observed melt rates (Fig. 8). The modeled daily snowmelt during this period was similar
14 for north- and south-facing slopes, likely because of higher melt rates but a smaller snow-covered area of the
15 south-facing slope in contrast to the north-facing slope during peak melt (Fig. 9). The model performance was
16 good according to SWE values (Table 3) and to snow cover extent (Fig. 6 and 7). The spatial variations of
17 snowpack isotopic content are significantly evidenced for north- and south-facing slopes, as also shown by
18 Carey and Quinton (2004), Dahlke and Lyon (2013) and Dietermann and Weiler (2013) in their high-gradient
19 catchments, whereas ambiguous findings exist for the spatial variation of the snowmelt isotopic signal. It is not
20 clear to which extent altitude is important, as Dietermann and Weiler (2013) stated that a potential elevation
21 effect is likely to be disturbed by melting processes (isotopic enrichment) depending on catchment morphology
22 during the ablation period. An altitudinal gradient was not considered in the present study, but possible effects
23 on IHS are discussed in Section 5.6. Beaulieu et al. (2012) detected elevation as a predictor, which explained
24 most of the variance they observed in snowmelt $\delta^{18}\text{O}$ from four distributed snow lysimeters. Moore (1989) and
25 Laudon et al. (2007) found no significant difference of $\delta^{18}\text{O}$ in their lysimeter outflows, likely due to the small
26 elevation gradient of their catchments which favours an isotopically homogenous snowpack, whereas
27 Unnikrishna et al. (2002) found a remarkable small-scale spatial variability. The difference of snowmelt (not
28 snowpack) isotopic signature between north- and south-facing slopes was clearly shown in the presented study.
29 The dataset is small, but reveals clear differences enforced by varying magnitudes and timing of melt processes
30 through solar radiation on the opposing slopes (cf. Fig. 5). Temporal snowmelt isotopic variability is greater for
31 the north-facing slope compared to the south-facing slope (Fig. 5), which was also pointed out by Carey and
32 Quinton (2004) in their subarctic catchment. Earlier homogenization of the snowpack isotopic profile and earlier
33 melt out are responsible for this phenomenon (cf. Dincer et al., 1970; Unnikrishna et al., 2002). Fractionation
34 processes controlled the ongoing homogenization of the snowpack between the two investigated melt events.
35 The isotopic homogenization of the snowpack on the south-facing slope started earlier in the melting period and
36 caused a smaller spatial and temporal variation compared the north-facing snowpack, as also reported by
37 Unnikrishna et al. (2002) and Dincer et al. (1970). However the differences between these investigated
38 snowpacks in the early melt season were larger than in the peak melt season. This affects IHS results, especially
39 because the snowmelt contributions from the south- and north-facing slope - with marked isotopic differences -
40 were distinct. Due to melt, fractionation processes proceeded and the snowpack became more homogenous



1 throughout the snowmelt season. However, inter-daily variations of snowpack isotopic content, especially for the
2 north-facing slope, were still observable during the peak melt period. The gradual isotopic enrichment of the
3 snowpack was also observable for snowmelt, as described by many others (Feng et al., 2002; Shanley et al.,
4 2002; Taylor et al., 2001; Taylor et al., 2002; Unnikrishna et al., 2002). Unnikrishna et al. (2002) described
5 significant temporal variations of snowmelt $\delta^{18}\text{O}$ during large snowmelt events (peak melt). However, these
6 findings could not be confirmed within in this study, probably due to the temporally limited data and should be
7 tested with a larger dataset.

8 **5.3 Validity of isotopic hydrograph separation**

9 The validity of IHS relies on several assumptions (Buttle, 1994; Klaus and McDonnell, 2013). The assumption –
10 the isotopic content of event and pre-event water differ significantly – was successfully proven, because
11 measured snowmelt isotopic values were markedly lower than pre-event baseflow values (cf. Table 2 and 4, Fig.
12 3). Spatio-temporal variations of event water isotopic content were accounted for by collecting daily and sub-
13 daily samples during both events throughout the freshet period and meltwater sampling at a north- and south-
14 facing slope, respectively. The spatially variable input of event water was considered by dividing the catchment
15 into two parts – a north- and a south-facing slope. This study supports the findings of Dahlke and Lyon (2013)
16 and Carey and Quinton (2004), emphasizing the highly variable snowpack/snowmelt isotopic content due to
17 enrichment in complex topography catchments. The temporal variability of event water isotopic content was
18 considered by bulk daily samples, which integrate the entire diurnal melting cycle. The spatio-temporal
19 variability of the isotopic content of pre-event water is a major limitation and could not be clearly identified due
20 to a lack of data and was therefore assumed to be constant. Small differences between pre-event and post-event
21 streamwater isotopic content support this assumption (Table 2). The assumption of soil water having the same
22 isotopic content as groundwater in time and space is quite critical. Some studies reveal no significant differences
23 (e.g. Laudon et al., 2007), whereas others do (e.g. Sklash and Farvolden 1979). Isotopic differences between
24 groundwater and soil water were not notable due to a lack of data. Furthermore it is not known to which amount
25 the vadose zone contributes to baseflow in the study area. Winter baseflow used in the analyses is assumed to
26 integrate mainly groundwater and partly soil water. Soil water could be hypothesized to have a negligible
27 contribution to baseflow during winter due to the recession of the soil storage in autumn and frozen soils in
28 winter. The assumption – no or minimal surface storage occurs – is plausible because water bodies like lakes or
29 wetlands do not exist in the study catchment and due to the steep topography detention storage may not be
30 relevant. The transit time of snowmelt was assumed to be less than 24 h. This short travel time is characteristic
31 for headwater catchments with (Lundquist et al., 2005): high in-channel flow velocities; steep hillslopes; a high
32 drainage density with snow-fed tributaries; thin soils; most snowmelt originating from the edge of the snow-line
33 (small average travel distances); partly frozen soil; and observed surface overland flow. The state-of-the-art
34 method (runCE) to include residence times of snowmelt in the event water reservoir proposed by Laudon et al.
35 (2002), was applied in several IHS studies (Beaulieu et al., 2012; Carey and Quinton, 2004; Petrone et al., 2007),
36 but was not feasible due to the short-term character and temporally limited data of the experimental design.

37 **5.4 Hydrograph separation results and inferred runoff generation processes**

38 High contributions from snowmelt to streamflow are common in high-elevation catchments. Daily contributions
39 between 35 and 75 % in the Rofen valley are comparable to the results of studies conducted in other



1 mountainous regions, mostly outside the European Alps. Beaulieu et al. (2012) estimated snowmelt contributions
2 ranging from 7 to 66 % at the seasonal scale for their 2.4 km² catchment and reported contributions of 34 and
3 62 %, for the early melt and peak melt, respectively. The hydrograph is dominated by pre-event water during
4 early melt in April (Fig. 10c), which is in accordance with the results obtained by other IHS studies (Beaulieu et
5 al., 2012; Laudon et al., 2004; Laudon et al., 2007; Moore, 1989). Initial snowmelt events flush the pre-event
6 water reservoir as snowmelt infiltrates into the soil and causes the pre-event water to exfiltrate and contribute to
7 the streamflow. As the soil and groundwater reservoir becomes gradually filled with new water (snowmelt), the
8 event water fraction in the stream increases. The system is also wetter during peak melt. The dominance of event
9 water in the hydrograph is interpreted as an outflow of pre-event water stored in the subsurface and the gradual
10 replenishment of event water. The higher water table – compared to the early melt period – could cause a
11 transmissivity feedback mechanism (Bishop, 1991). This is a common mechanism in catchments with glacial till
12 (Bishop et al., 2011) and characterises higher transmissivities and hence increasing lateral flow velocities
13 towards to the surface. Runoff generation is spatially very variable in the study area. There are areas (meadow
14 patches between rock fields) where saturation excess overland flow is dominant (observed mainly at plots S1, S2
15 and Wind) and areas (with larger rocks and debris) where rapid shallow subsurface flow can be assumed (plot
16 N2). Catchment morphology controls various hydrologic processes and hence the shape of the hydrograph.
17 Upslope residence times of snowmelt are usually smaller due to thinner soils (observed during the field work),
18 steeper slopes (Sueker et al., 2000) and higher contributing areas of glaciers with impermeable ice (Behrens,
19 1978) and would be indicators for the more flashy hydrograph during the peak melt season. The snowmelt
20 contribution increased as the freshet period progressed and peaked with high contributions at the beginning of
21 June. Beaulieu et al. (2012) and Sueker et al. (2000) reported comparable results for their physically similar
22 catchments during peak melt with 62 and up to 76 % event water contributions to streamflow, respectively. At
23 the event-scale comparable studies are rare. Engel et al. (2015) report a maximum daily snowmelt contribution
24 estimated with a three-component hydrograph separation of 33 % for an 11 km² catchment southwest of the
25 Rofen valley with similar physiographic characteristics, but on the southern side of the main Alpine ridge. It
26 should be mentioned that in their study, runoff was fed by three components (snowmelt, glacier melt and
27 groundwater) and lower snowmelt contributions were prevalent because most of the catchment area (69 %) was
28 snow-free.

29 **5.5 Impact of spatial varying snowmelt and its $\delta^{18}\text{O}$ content on IHS (Assessment of weighting approaches)**

30 Klaus and McDonnell (2013) stress in their review paper the need for investigating the effects of the spatially
31 varying snowmelt and its isotopic content on IHS. The present study quantified the impact of spatially varying
32 snowmelt isotopic content between north- and south facing slopes on IHS results for the first time. The
33 difference in volumetric snowmelt contribution to streamflow at the event-scale determined using the five
34 different weighting methods for IHS is maximal 24 % (NORTH approach vs. SOUTH approach). The data show
35 that the variations between the weighting approaches (VWS, VWO and VWE) are higher throughout the early
36 melt season (Table 6), because small-scale variability of snowmelt and its isotopic content are more pronounced
37 in the early melt season. Thus the influence of spatial variability of snowmelt and its isotopic content on the
38 event water fraction calculated with IHS is larger during this time. Melt rates strongly differ between the south-
39 and the north-facing slope (Fig. 9), which was deceptively gathered by manually measured SWE, likely due to
40 micro-topographic effects. As the contributions from both slopes are used in Eq. (3), they strongly influence the



1 applied weighting technique. The weighting method SOUTH (or NORTH) represents the most extreme scenario
2 in which only one sampling site was deployed in the IHS analysis. Because snowmelt is more depleted in $\delta^{18}\text{O}$
3 and closer to pre-event water isotopic content on the south-facing slope during peak melt, this scenario has the
4 greatest effect on IHS and leads to the strongest deviation in estimated snowmelt fractions (up to 15 %
5 overestimation compared to the VWS approach). Similar to the VWE method, snowmelt isotopic data was not
6 volume-weighted in other studies (e.g. Engel et al., 2015) since snowmelt data was not available. This has a
7 more distinct effect on IHS during the early melt season because of the higher spatio-temporal variability in
8 snowmelt and its isotopic content compared to the peak melt season and led to a deviation in the snowmelt
9 fraction of 2 % and 3 % compared to the VWS and VWO approach, respectively. Although the differences seem
10 to be small, it should be mentioned that differing snowmelt and isotopic values offset each other in this particular
11 case, which led to the relatively small differences in estimated snowmelt fractions (Table 6). Nevertheless the
12 results of VWS are more correct for the right reason, because single observed plot-scale melt rates do not
13 represent distributed snowmelt contribution at the catchment-scale. Therefore one can hypothesize that
14 distributed simulated melt rates enhance the reliability and feasibility of IHS, whereas plot-scale weighting
15 implements a very high error caused by the difficulty in finding locations that represent the melt rate of a slope
16 in complex terrain. The IHS results of this study are more sensitive to the spatial variability of snowmelt $\delta^{18}\text{O}$,
17 than spatial variations of snowmelt rates (Table 6). This is even more pronounced for the peak melt period,
18 because snowmelt rates were similar for the north- and south-facing slope, probably due to an isothermal snow
19 cover throughout the catchment.

20 **5.6 Limitations of the study**

21 Collecting water samples in high-elevation terrain is challenging due to limited access and high exposure to risk
22 (e.g. avalanches), limiting especially high-frequency sampling. Hence some limitations are inherent in the
23 presented study. Potential elevation effects on snowmelt isotopic content were not tested. The opposing sampling
24 sites (S1-N1 and S2-N2) were at the same elevation (Fig. 1). It was assumed that the differences of north- and
25 south-facing slopes were significantly greater than a possible altitudinal gradient of snowmelt isotopic content.
26 This hypothesis was not tested, but assumed to be valid based on the results of other studies (Dietermann and
27 Weiler, 2013). However, accounting for a potential altitudinal gradient (decrease of snowmelt $\delta^{18}\text{O}$ with
28 elevation) would lead to more depleted isotopic signatures of event water and hence to lower event water
29 fractions. A disadvantage is that no snow survey was conducted prior to the onset of snowmelt (peak
30 accumulation) to estimate spatial variability in bulk snow $\delta^{18}\text{O}$. Because snowmelt is used for applying IHS, it is
31 not clear to which degree the spatial variability of the snowpack isotopic content is important. Two-component
32 isotopic hydrograph separation was successfully applied using the end-members snowmelt and baseflow, but
33 potential contributions of glacier melt were neglected. Because glaciers in the catchment were still covered by
34 snow during the peak melt season, a significant contribution from ice melt was therefore assumed to be unlikely.
35 Nevertheless negligible amounts of basal meltwater could originate from temperate glaciers. No samples could
36 be collected during the recession of the hydrograph (at night). Despite spatial variability of the event water signal
37 was the focus of the study, only temporal variability was considered in the Genereux-based uncertainty.
38 Furthermore, model results and observed discharges were assumed to be free of error in the analyses. As pointed
39 out, instrumentation and accessibility are major problems for high-elevation studies and their sampling
40 strategies. For this study it turned out that composite snowmelt samples were easier to collect, representing the



1 day-integrated melt signal. A denser network of melt collectors would be desirable, as well as a snow lysimeter
2 to gain high-frequency data automatically. Representative samples of the elevation zones and different
3 vegetation belts could be important too, especially in partly forested catchments with a distinct relief (cf.
4 Unnikrishna et al., 2002).

5 **6 Conclusions**

6 The presented study provides new insights into the variability of snowmelt isotopic content and highlights its
7 impact on IHS in a high-elevation environment. The spatial variability of snowmelt isotopic signatures was
8 extensively considered by experimental investigations on south- and north-facing slopes to define tracer
9 concentrations of the snowmelt end-member with greater accuracy. This study clearly shows that distributed
10 snowmelt rates simulated by a model, fed with meteorological data from local automatic weather stations, affect
11 the weighting of the event water isotopic signal, and hence the estimation of snowmelt fraction in the stream by
12 IHS. The study provides a variety of relevant findings that are important for hydrologic research in high-alpine
13 environments: a distinct snowmelt variability between north- and south-facing slopes was shown for this
14 complex terrain, especially during the early melt season; isotopic signatures of snowmelt water were
15 significantly different between north-facing and south-facing slopes, which resulted in a pronounced effect on
16 estimating snowmelt contributions to streamflow with IHS; differences in the estimated snowmelt fraction due to
17 the weighting methods used for IHS were quantified by up to 24 %. It became evident that it is hardly possible to
18 characterize the event water signature of larger slopes based on plot-scale snowmelt measurements. Applying
19 distributed modelling reduced the uncertainty of the spatial snowmelt variability inherent in point-scale
20 observations. Hence, applying the VWS method provided more reasonable results than the VWO method.
21 Sampling north- and south-facing slopes is of major importance in conducting snowmelt-based IHS in
22 mountainous catchments with complex topography in which a non-uniform input of snowmelt can be expected.
23 Therefore, it has to be pointed out that the selection of sampling sites has a major effect on IHS results. Sampling
24 at least north-facing and south-facing slopes in complex terrain and using distributed melt rates to weight the
25 snowmelt isotopic content of the differing exposures is therefore highly recommended for applying snowmelt-
26 based IHS.

27

28 *Acknowledgments.* The authors wish to thank the Institute of Atmospheric and Cryospheric Sciences of the University of
29 Innsbruck, the Zentralanstalt für Meteorologie und Geodynamik, the Hydrographic Service of Tyrol and the TIWAG-Tiroler
30 Wasserkraft AG for providing hydrological and meteorological data, the Amt der Tiroler Landesregierung for providing the
31 DEM, as well as many individuals who have helped to collect data in the field.

32 **References**

33 Ahluwalia, R. S., Rai, S. P., Jain, S. K., Kumar, B., and Dobhal, D. P.: Assessment of snowmelt runoff
34 modelling and isotope analysis: a case study from the western Himalaya, India, *Annals of Glaciology*, 54, 299-
35 304, doi:10.3189/2013AoG62A133, 2013.
36 APCC: Austrian Assessment Report (AAR14). Summary for Policymakers (SPM), Austrian Panel on Climate
37 Change, Vienna, Austria, 2014.



- 1 Árnason, B., Buason, T., Martinec, J., and Theodorson, P.: Movement of water through snowpack traced by
2 deuterium and tritium. In: The role of snow and ice in hydrology. Proc. Banff Symp., UNESCO-WMO-IAHS
3 (Ed.), IAHS Publ. No., 107, 1973.
- 4 Beaulieu, M., Schreier, H., and Jost, G.: A shifting hydrological regime: a field investigation of snowmelt runoff
5 processes and their connection to summer base flow, Sunshine Coast, British Columbia, Hydrological Processes,
6 26, 2672-2682, doi:10.1002/hyp.9404, 2012.
- 7 Behrens, H., Moser, H., Oerter, H., Rauert, W., Stichler, W. and Ambach, W.: Models for the runoff from a
8 glaciated catchment area using measurements of environmental isotope contents, 1978, 829-846.
- 9 Birkel, C. and Soulsby, C.: Advancing tracer-aided rainfall-runoff modelling: a review of progress, problems and
10 unrealised potential, Hydrological Processes, 29, 5227-5240, doi:10.1002/hyp.10594, 2015.
- 11 Birkel, C., Tetzlaff, D., Dunn, S. M., and Soulsby, C.: Using time domain and geographic source tracers to
12 conceptualize streamflow generation processes in lumped rainfall-runoff models, Water Resources Research, 47,
13 n/a-n/a, doi:10.1029/2010WR009547, 2011.
- 14 Bishop, K.: Episodic increase in stream acidity, catchment flow pathways and hydrograph separation, 1991.
- 15 Bishop, K., Seibert, J., Nyberg, L., and Rodhe, A.: Water storage in a till catchment. II: Implications of
16 transmissivity feedback for flow paths and turnover times, Hydrological Processes, 25, 3950-3959,
17 doi:10.1002/hyp.8355, 2011.
- 18 Braithwaite, R. J. and Olesen, O. B.: Calculation of glacier ablation from air temperature, West Greenland. In:
19 Glacier Fluctuations and Climatic Change, Glaciology and Quaternary Geology, Oerlemans, J. (Ed.), Kluwer
20 Academic Publisher, Dordrecht, 1989.
- 21 Buttle, J. M.: Isotope hydrograph separations and rapid delivery of pre-event water from drainage basins,
22 Progress in Physical Geography, 18, 16-41, doi:10.1177/030913339401800102, 1994.
- 23 Capell, R., Tetzlaff, D., and Soulsby, C.: Can time domain and source area tracers reduce uncertainty in rainfall-
24 runoff models in larger heterogeneous catchments?, Water Resources Research, 48, n/a-n/a,
25 doi:10.1029/2011WR011543, 2012.
- 26 Carey, S. K. and Quinton, W. L.: Evaluating snowmelt runoff generation in a discontinuous permafrost catchment
27 using stable isotope, hydrochemical and hydrometric data, Nordic Hydrology, 35, 309-324, 2004.
- 28 Clark, I. D. and Fritz, P.: Environmental Isotopes in Hydrogeology, Lewis Publishers, New York, 1997.
- 29 CLC: Corine Land Cover 2006 raster data. European Environment Agency. The European Topic Centre on Land
30 Use and Spatial Information. 2006.
- 31 Cooper, L. W.: Isotopic fractionation in snow cover. In: Isotope tracers in catchment hydrology, Kendall, C. and
32 McDonnell, J. J. (Eds.), Elsevier Science, Amsterdam, Netherlands, 2006.
- 33 Corripio, J. G.: Vectorial algebra algorithms for calculating terrain parameters from DEMs and the position of
34 the sun for solar radiation modelling in mountainous terrain, International Journal of Geographical Information
35 Science, 17, 1-23, 2003.
- 36 Dahlke, H. E. and Lyon, S. W.: Early melt season snowpack isotopic evolution in the Tarfala valley, northern
37 Sweden, Annals of Glaciology, 54, 149-156, doi:10.3189/2013AoG62A232, 2013.
- 38 Dietermann, N. and Weiler, M.: Spatial distribution of stable water isotopes in alpine snow cover, Hydrology
39 and Earth System Sciences, 17, 2657-2668, doi:10.5194/hess-17-2657-2013, 2013.
- 40 Dinçer, T., Payne, B. R., Florkowski, T., Martinec, J., and Tongiorgi, E.: Snowmelt runoff from measurements
41 of tritium and oxygen-18, Water Resources Research, 6, 110-124, doi:10.1029/WR006i001p00110, 1970.



- 1 Engel, M., Penna, D., Bertoldi, G., Dell'Agnese, A., Soulsby, C., and Comiti, F.: Identifying run-off
2 contributions during melt-induced run-off events in a glacierized alpine catchment, *Hydrological Processes*, doi:
3 10.1002/hyp.10577, 2015. n/a-n/a, doi:10.1002/hyp.10577, 2015.
- 4 Feng, X., Taylor, S., Renshaw, C. E., and Kirchner, J. W.: Isotopic evolution of snowmelt 1. A physically based
5 one-dimensional model, *Water Resources Research*, 38, 35-31-35-38, doi:10.1029/2001WR000814, 2002.
- 6 Genereux, D.: Quantifying uncertainty in tracer-based hydrograph separations, *Water Resources Research*, 34,
7 915-919, doi:10.1029/98WR00010, 1998.
- 8 Greuell, W., Knap, W. H., and Smeets, P. C.: Elevational changes in meteorological variables along a
9 midlatitude glacier during summer, *Journal of Geophysical Research: Atmospheres*, 102, 25941-25954,
10 doi:10.1029/97JD02083, 1997.
- 11 Gruber, S.: A mass-conserving fast algorithm to parameterize gravitational transport and deposition using digital
12 elevation models, *Water Resources Research*, 43, n/a-n/a, doi:10.1029/2006WR004868, 2007.
- 13 Haeblerli, W.: Untersuchungen zur Verbreitung von Permafrost zwischen Flüelapass und Piz Grialetsch
14 (Graubünden), 1975.
- 15 Hanzer, F., Helfricht, K., Marke, T., and Strasser, U.: Multi-level spatiotemporal validation of snow/ice mass
16 balance and runoff modeling in glacierized catchments, *The Cryosphere Discuss.*, 2016, 1-37, doi:10.5194/tc-
17 2016-58, 2016.
- 18 Hanzer, F., Marke, T., and Strasser, U.: Distributed, explicit modeling of technical snow production for a ski
19 area in the Schladming region (Austrian Alps), *Cold Regions Science and Technology*, 108, 113-124,
20 doi:http://dx.doi.org/10.1016/j.coldregions.2014.08.003, 2014.
- 21 Helfricht, K.: Analysis of the spatial and temporal variation of seasonal snow accumulation in Alpine catchments
22 using airborne laser scanning. Basic research for the adaptation of spatially distributed hydrological models to
23 mountain regions, PhD, University of Innsbruck, Innsbruck, 134 pp., 2014.
- 24 Hock, R.: Temperature index melt modelling in mountain areas, *Journal of Hydrology*, 282, 104-115,
25 doi:10.1016/S0022-1694(03)00257-9, 2003.
- 26 Hooper, R. P. and Shoemaker, C. A.: A Comparison of Chemical and Isotopic Hydrograph Separation, *Water
27 Resources Research*, 22, 1444-1454, doi:10.1029/WR022i010p01444, 1986.
- 28 Huth, A. K., Leydecker, A., Sickman, J. O., and Bales, R. C.: A two-component hydrograph separation for three
29 high-elevation catchments in the Sierra Nevada, California, *Hydrological Processes*, 18, 1721-1733,
30 doi:10.1002/hyp.1414, 2004.
- 31 IPCC: Summary for Policymakers. *Climate Change 2013: The Physical Science Basis. Contribution of Working
32 Group I to the Fifth Assessment Report of the Intergovernmental Panel on Climate Change*, Cambridge, United
33 Kingdom and New York, NY, USA., 2013.
- 34 Klaus, J. and McDonnell, J. J.: Hydrograph separation using stable isotopes: Review and evaluation, *Journal of
35 Hydrology*, 505, 47-64, doi:10.1016/j.jhydrol.2013.09.006, 2013.
- 36 Laudon, H., Hemond, H. F., Krouse, R., and Bishop, K. H.: Oxygen 18 fractionation during snowmelt:
37 Implications for spring flood hydrograph separation, *Water Resources Research*, 38, 40-41-40-10,
38 doi:10.1029/2002WR001510, 2002.
- 39 Laudon, H., Seibert, J., Köhler, S., and Bishop, K.: Hydrological flow paths during snowmelt: Congruence
40 between hydrometric measurements and oxygen 18 in meltwater, soil water, and runoff, *Water Resources
41 Research*, 40, n/a-n/a, doi:10.1029/2003WR002455, 2004.



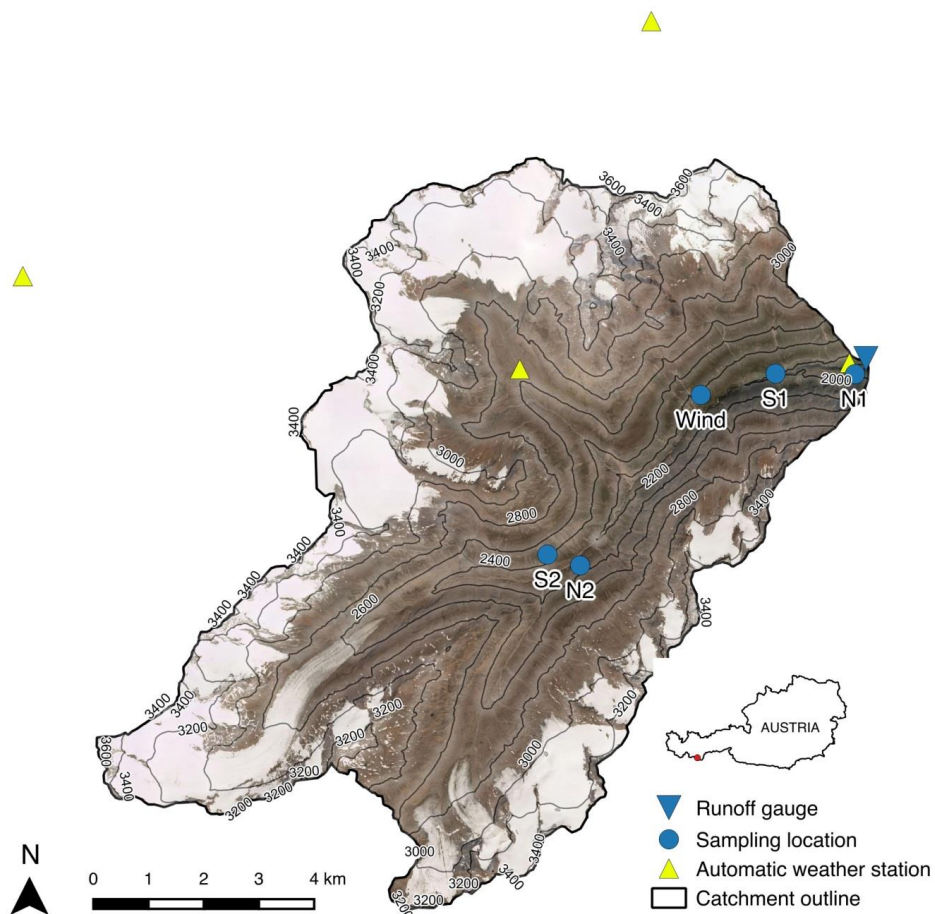
- 1 Laudon, H., Sjöblom, V., Buffam, I., Seibert, J., and Mörtz, M.: The role of catchment scale and landscape
2 characteristics for runoff generation of boreal streams, *Journal of Hydrology*, 344, 198-209,
3 doi:10.1016/j.jhydro.2007.07.010, 2007.
- 4 Lee, J., Feng, X., Faiia, A. M., Posmentier, E. S., Kirchner, J. W., Osterhuber, R., and Taylor, S.: Isotopic
5 evolution of a seasonal snowcover and its melt by isotopic exchange between liquid water and ice, *Chemical*
6 *Geology*, 270, 126-134, doi:10.1016/j.chemgeo.2009.11.011, 2010.
- 7 Liston, G. E. and Elder, K.: A Distributed Snow-Evolution Modeling System (SnowModel), *Journal of*
8 *Hydrometeorology*, 7, 1259-1276, doi:10.1175/JHM548.1, 2006.
- 9 Liu, F., Williams, M. W., and Caine, N.: Source waters and flow paths in an alpine catchment, Colorado Front
10 Range, United States, *Water Resources Research*, 40, 1-16, doi:10.1029/2004WR003076, 2004.
- 11 Lundquist, J. D. and Cayan, D. R.: Seasonal and Spatial Patterns in Diurnal Cycles in Streamflow in the Western
12 United States, *Journal of Hydrometeorology*, 3, 591-603, doi:10.1175/1525-
13 7541(2002)003<0591:SASPID>2.0.CO;2, 2002.
- 14 Lundquist, J. D., Dettinger, M. D., and Cayan, D. R.: Snow-fed streamflow timing at different basin scales: Case
15 study of the Tuolumne River above Hetch Hetchy, Yosemite, California, *Water Resources Research*, 41, n/a-n/a,
16 doi:10.1029/2004WR003933, 2005.
- 17 Marke, T.: Development and Application of a Model Interface to couple Regional Climate Models with Land
18 Surface Models for Climate Change Risk Assessment in the Upper Danube Watershed, Dissertation der Fakultät
19 für Geowissenschaften, Digitale Hochschulschriften der LMU München, München, 2008.
- 20 Marke, T., Strasser, U., Hanzer, F., Stötter, J., Wilcke, R. A. I., and Gobiet, A.: Scenarios of Future Snow
21 Conditions in Styria (Austrian Alps), *Journal of Hydrometeorology*, 16, 261-277, doi:10.1175/JHM-D-14-
22 0035.1, 2015.
- 23 Martinec, J., Siegenthaler, U., Oeschger, H., and Tongiorgi, E.: New insights into the run-off mechanism by
24 environmental isotopes. In: *Isotope techniques in groundwater hydrology, Symposium, P. o. a. I. (Ed.)*, IAEA,
25 Vienna, Austria, 1974.
- 26 Mast, A. M., Kendall, K., Campbell, D. H., Clow, D. W., and Back, J.: Determination of hydrologic pathways in
27 an alpine-subalpine basin using isotopic and chemical tracers, Loch Vale Watershed, Colorado, Usa. In: *IAHS*
28 *Publ. Ser. Proc. Rep. Int. Assoc. Hydrol. SCI.*, 1995.
- 29 Maulé, C. P. and Stein, J.: Hydrologic Flow Path Definition and Partitioning of Spring Meltwater, *Water*
30 *Resources Research*, 26, 2959-2970, doi:10.1029/WR026i012p02959, 1990.
- 31 Moore, R. D.: Tracing runoff sources with deuterium and oxygen-88 during spring melt in a headwater
32 catchment, southern Laurentians, Quebec, *Journal of Hydrology*, 112, 135-148,
33 doi:http://dx.doi.org/10.1016/0022-1694(89)90185-6, 1989.
- 34 Pellicciotti, F., Brock, B., Strasser, U., Burlando, P., Funk, M., and Corripio, J.: An enhanced temperature-index
35 glacier melt model including the shortwave radiation balance: development and testing for Haut Glacier d'Arolla,
36 Switzerland, *Journal of Glaciology*, 51, 573-587, 2005.
- 37 Penna, D., Engel, M., Mao, L., Dell'Agnese, A., Bertoldi, G., and Comiti, F.: Tracer-based analysis of spatial and
38 temporal variations of water sources in a glacierized catchment, *Hydrology and Earth System Sciences*, 18,
39 5271-5288, doi:10.5194/hess-18-5271-2014, 2014.



- 1 Petrone, K., Buffam, I., and Laudon, H.: Hydrologic and biotic control of nitrogen export during snowmelt: A
2 combined conservative and reactive tracer approach, *Water Resources Research*, 43, 1-13,
3 doi:10.1029/2006WR005286, 2007.
- 4 Pinder, G. F. and Jones, J. F.: Determination of the ground-water component of peak discharge from the
5 chemistry of total runoff, *Water Resources Research*, 5, 438-445, doi:10.1029/WR005i002p00438, 1969.
- 6 Pomeroy, J. W., Toth, B., Granger, R. J., Hedstrom, N. R., and Essery, R. L. H.: Variation in Surface Energetics
7 during Snowmelt in a Subarctic Mountain Catchment, *Journal of Hydrometeorology*, 4, 702-719,
8 doi:10.1175/1525-7541(2003)004<0702:VISED5>2.0.CO;2, 2003.
- 9 Rohrer, M. B.: *Die Schneedecke im Schweizer Alpenraum und ihre Modellierung*, ETH, Zürich, 1992.
- 10 Schuler, T.: Investigation of water drainage through an alpine glacier by tracer experiments and numerical
11 modeling., 2002.
- 12 Seibert, J. and McDonnell, J. J.: On the dialog between experimentalist and modeler in catchment hydrology:
13 Use of soft data for multicriteria model calibration, *Water Resources Research*, 38, 23-21-23-14,
14 doi:10.1029/2001WR000978, 2002.
- 15 Shanley, J. B., Kendall, C., Smith, T. E., Wolock, D. M., and McDonnell, J. J.: Controls on old and new water
16 contributions to stream flow at some nested catchments in Vermont, USA, *Hydrological Processes*, 16, 589-609,
17 doi:10.1002/hyp.312, 2002.
- 18 Sklash, M. G. and Farvolden, R. N.: The role of groundwater in storm runoff, *Journal of Hydrology*, 43, 45-65,
19 doi:10.1016/0022-1694(79)90164-1, 1979.
- 20 Sklash, M. G., Farvolden, R. N., and Fritz, P.: A conceptual model of watershed response to rainfall, developed
21 through the use of oxygen-18 as a natural tracer, *Canadian Journal of Earth Sciences*, 13, 271-283,
22 doi:10.1139/e76-029, 1976.
- 23 Stichler, W.: *Snowcover and Snowmelt Processes Studied by Means of Environmental Isotopes*. In: *Seasonal*
24 *Snowcovers: Physics, Chemistry, Hydrology*, Jones, H. G. and Orville-Thomas, W. J. (Eds.), D. Reidel
25 Publishing Company, Dordrecht, Holland, 1987.
- 26 Strasser, U.: *Modelling of the mountain snow cover in the Berchtesgaden National Park*, Research Rep., 2008.
- 27 Strasser, U., Bernhardt, M., Weber, M., Liston, G. E., and Mauser, W.: Is snow sublimation important in the
28 alpine water balance?, *The Cryosphere*, 2, 53-66, doi:10.5194/tc-2-53-2008, 2008.
- 29 Strasser, U., Corripio, J., Pellicciotti, F., Burlando, P., Brock, B., and Funk, M.: Spatial and temporal variability
30 of meteorological variables at Haut Glacier d'Arolla (Switzerland) during the ablation season 2001:
31 Measurements and simulations, *Journal of Geophysical Research: Atmospheres*, 109, n/a-n/a,
32 doi:10.1029/2003JD003973, 2004.
- 33 Strasser, U., Warscher, M., and Liston, G. E.: Modeling Snow-Canopy Processes on an Idealized Mountain,
34 *Journal of Hydrometeorology*, 12, 663-677, doi:10.1175/2011JHM1344.1, 2011.
- 35 Sueker, J. K., Ryan, J. N., Kendall, C., and Jarrett, R. D.: Determination of hydrologic pathways during
36 snowmelt for alpine/subalpine basins, Rocky Mountain National Park, Colorado, *Water Resources Research*, 36,
37 63-75, doi:10.1029/1999WR900296, 2000.
- 38 Taylor, S., Feng, X., Kirchner, J. W., Osterhuber, R., Klaue, B., and Renshaw, C. E.: Isotopic evolution of a
39 seasonal snowpack and its melt, *Water Resources Research*, 37, 759-769, doi:10.1029/2000WR900341, 2001.
- 40 Taylor, S., Feng, X., Williams, M., and McNamara, J.: How isotopic fractionation of snowmelt affects
41 hydrograph separation, *Hydrological Processes*, 16, 3683-3690, doi:10.1002/hyp.1232, 2002.

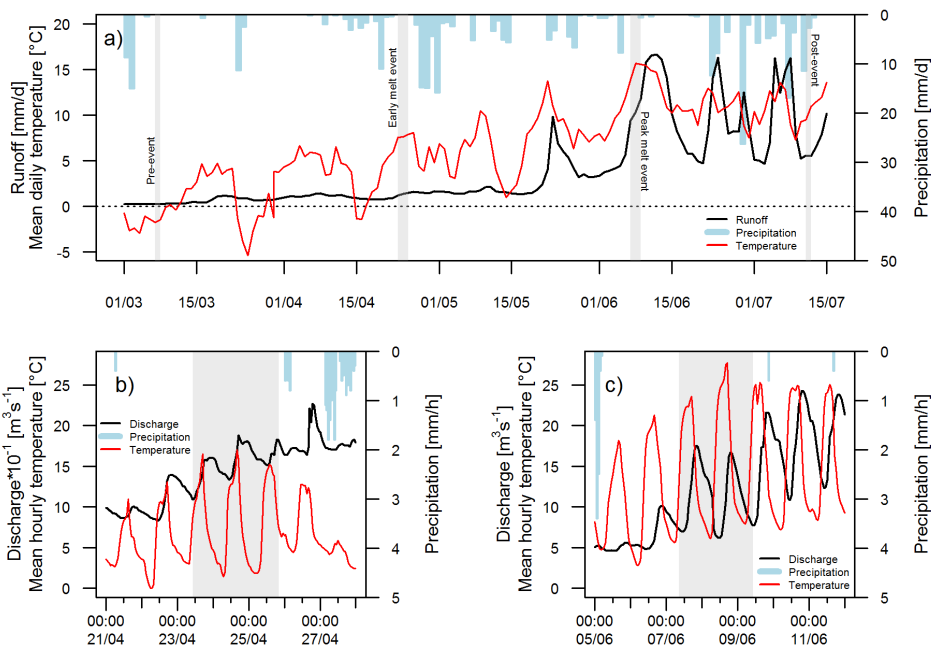


- 1 Uhlenbrook, S. and Leibundgut, C.: Process-oriented catchment modelling and multiple-response validation,
- 2 Hydrological Processes, 16, 423-440, doi:10.1002/hyp.330, 2002.
- 3 Unnikrishna, P. V., McDonnell, J. J., and Kendall, C.: Isotope variations in a Sierra Nevada snowpack and their
- 4 relation to meltwater, 260, 38-57, 2002.
- 5 Warscher, M., Strasser, U., Kraller, G., Marke, T., Franz, H., and Kunstmann, H.: Performance of complex snow
- 6 cover descriptions in a distributed hydrological model system: A case study for the high Alpine terrain of the
- 7 Berchtesgaden Alps, Water Resources Research, 49, 2619-2637, doi:10.1002/wrcr.20219, 2013.
- 8 Weingartner, R. and Aschwanden, H.: Discharge regime - the basis for the estimation of average flows. In:
- 9 Hydrological Atlas of Switzerland, 1992.
- 10 Williams, M. W., Seibold, C., and Chowanski, K.: Storage and release of solutes from a subalpine seasonal
- 11 snowpack: soil and stream water response, Niwot Ridge, Colorado, Biogeochemistry, 95, 77-94,
- 12 doi:10.1007/s10533-009-9288-x, 2009.
- 13 Zappa, M.: Objective quantitative spatial verification of distributed snow cover simulations—an experiment for
- 14 the whole of Switzerland, Hydrological Sciences Journal, 53, 179-191, doi:10.1623/hysj.53.1.179, 2008.
- 15 Zhou, S., Nakawo, M., Hashimoto, S., and Sakai, A.: The effect of refreezing on the isotopic composition of
- 16 melting snowpack, Hydrological Processes, 22, 873-882, doi:10.1002/hyp.6662, 2008.
- 17



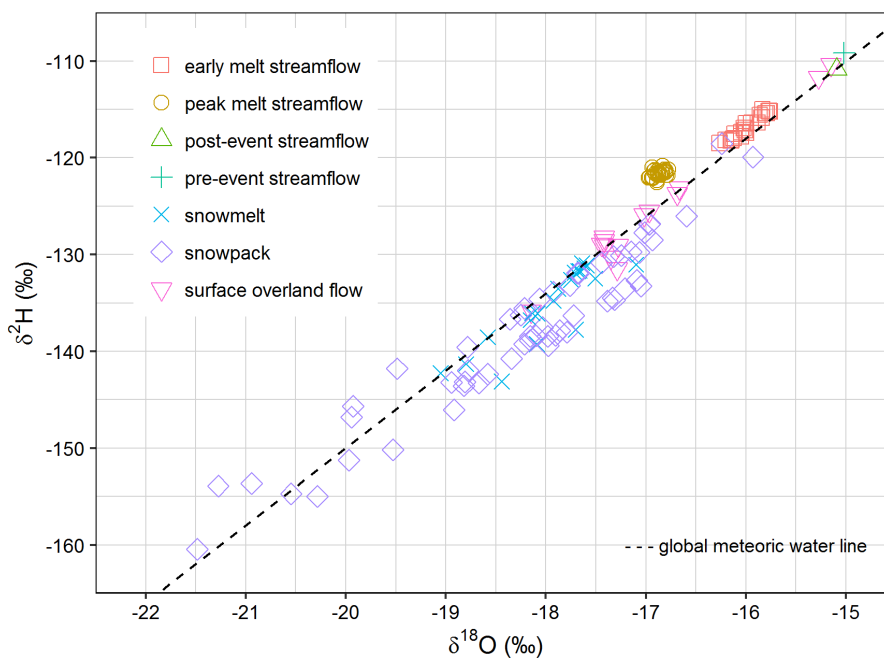
1

2 **Figure 1: Study area (Rofen valley) with underlying orthophoto, sampling and measurement locations.**



1
 2 **Figure 2: (a) Daily precipitation, air temperature, and discharge during the complete study period; Hourly hydro-**
 3 **climatic data of a 7-day period around the (b) early melt and (c) peak melt event. Data was measured at the outlet**
 4 **of the catchment. Grey-shaded areas indicate the investigated events.**

5

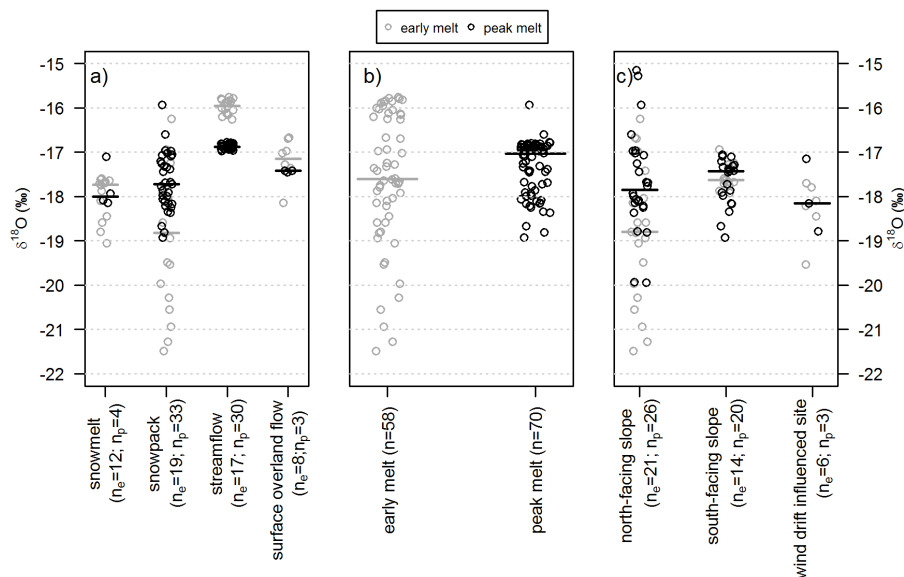


6



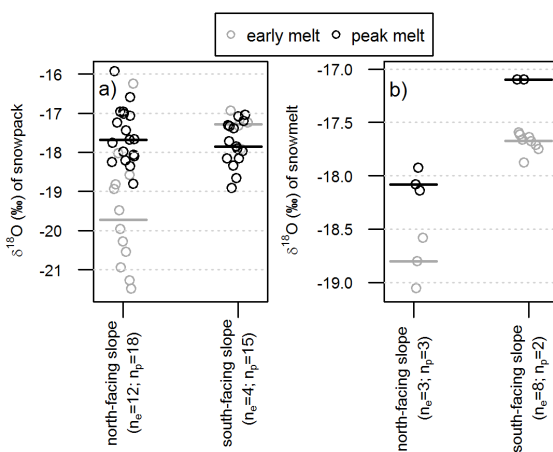
1 **Figure 3: Relationship between $\delta^2\text{H}$ and $\delta^{18}\text{O}$ values of water sources sampled during the snowmelt season 2014 in the**
 2 **Rofen valley, Austrian Alps.**

3



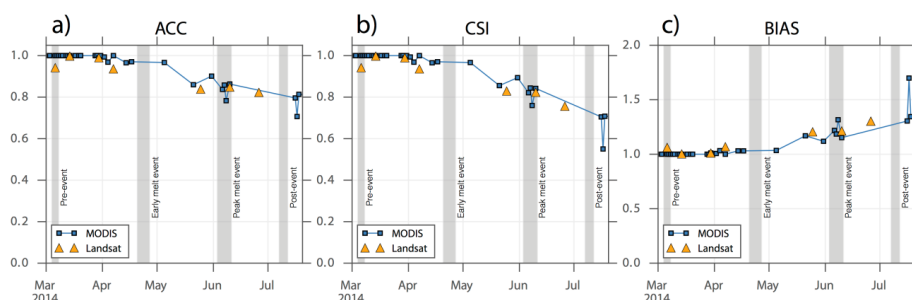
4

5 **Figure 4: 1-D scatterplots for $\delta^{18}\text{O}$ of collected water samples split into (a) water sources, (b) stage of snowmelt and (c)**
 6 **spatial origin. Grey circles indicate early melt samples and black circles are for peak melt samples. The grey and**
 7 **black line represents the median of early and peak melt data, respectively. N_e is the number of early melt samples and**
 8 **n_p is the number of peak melt samples.**



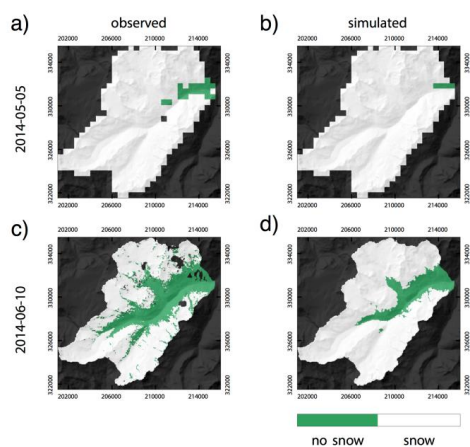
9

10 **Figure 5: 1-D scatterplots for $\delta^{18}\text{O}$ of (a) snowpack and (b) snowmelt of north- and south-facing slopes. Grey circles**
 11 **indicate early melt samples and black circles are for peak melt samples. The grey and black line indicates the median**
 12 **of the early and peak melt data, respectively. N_e is the number of early melt samples and n_p is the number of peak**
 13 **melt samples.**



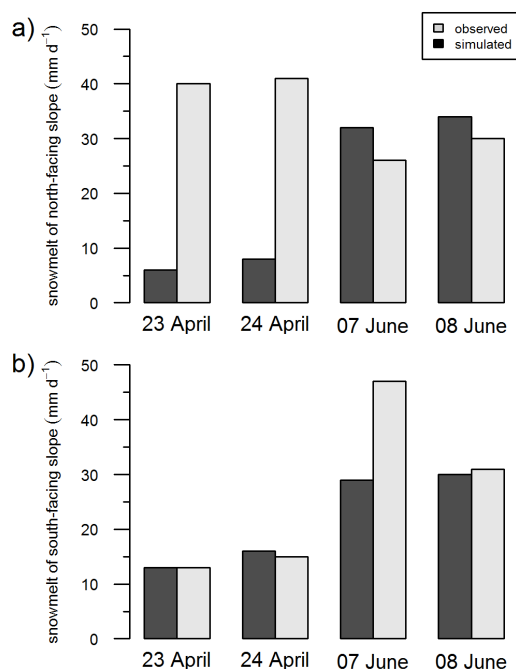
1
 2 **Figure 6: Performance measures (a) Accuracy (ACC), (b) Critical Success Index (CSI), and (c) BIAS as calculated by**
 3 **comparing AMUNDSEN simulation results with satellite-derived (MODIS/Landsat) snow maps.**

4



5
 6 **Figure 7: Comparison of observed and simulated snow distributions for (a, b) May 5 (MODIS scene) and (c, d)**
 7 **June 10, 2014 (Landsat scene).**

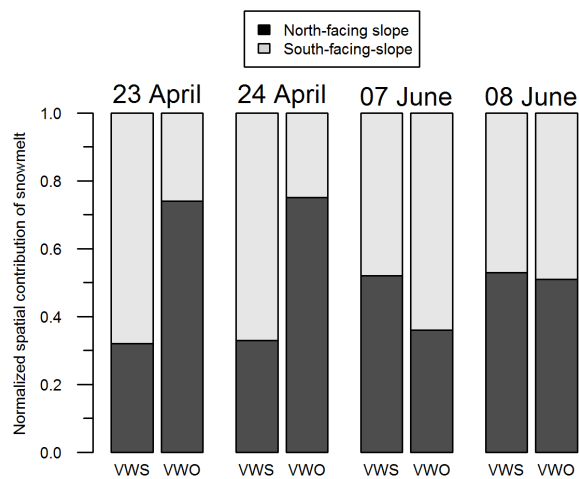
8



1

2 **Figure 8: Differences between the observed (plot scale) and simulated (catchment scale) daily snowmelt on (a) the**
 3 **north-facing and (b) the south-facing slope for the early melt (23/24 April) and peak melt (07/08 June).**

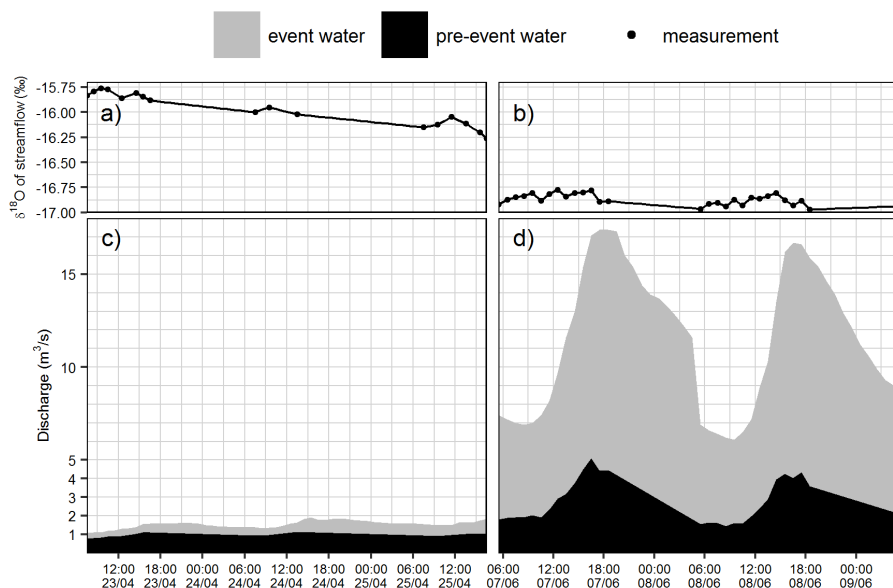
4



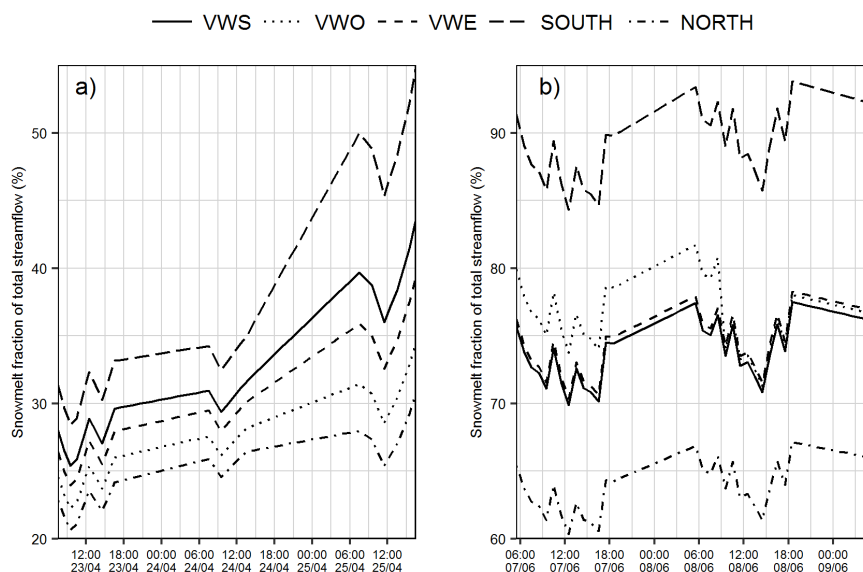
5

6 **Figure 9: Comparison of the spatial contribution of weighting approaches. VWS: volume-weighted with simulated**
 7 **(areal) melt rates. VWO: volume-weighted with observed (plot-scale) melt rates.**

8



1
 2 **Figure 10: Linearly interpolated stream isotopic content of Rofenache for (a) the early melt and (b) the peak melt**
 3 **event. Dots indicate measurements. Event and pre-event water contributions during (c) the early melt and (d) the**
 4 **peak melt event calculated with the VWS approach.**
 5



6
 7 **Figure 11: Comparison of weighting techniques used for estimating snowmelt fraction with IHS during (a) early melt**
 8 **and (b) peak melt. Scale of Y-axis in b) differs from that in a).**
 9
 10 **Table 1: Average isotopic content of snowpack and snowmelt with standard deviation for north- and south-facing**
 11 **slopes during the early and the peak melt event. Values are averages of three consecutive days.**



	North-facing slope		South-facing slope	
	Snowpack $\delta^{18}\text{O}$ (‰)	Snowmelt $\delta^{18}\text{O}$ (‰)	Snowpack $\delta^{18}\text{O}$ (‰)	Snowmelt $\delta^{18}\text{O}$ (‰)
Early melt event	-19.7±0.6 (n=12)	-18.8±0.2 (n=3)	-17.3±0.3 (n=4)	-17.4±0.2 (n=8)
Peak melt event	-17.6±0.4 (n=18)	-17.9±0.1 (n=3)	-17.9±0.1 (n=15)	-17.1±0.0 (n=2)

1

2

3 **Table 2: Descriptive statistics of streamflow isotopic content (Rofenache) during events of the snowmelt season 2014.**
4 Data is sampled at the outlet of the basin.

	Pre-event	Early melt	Peak melt	Post-event
Date	07/03	23/04 – 25/04	07/06 – 09/06	11/07
Average ($\delta^{18}\text{O}$ ‰)	-15.02	-15.97	-16.87	-15.09
Standard deviation ($\delta^{18}\text{O}$ ‰)	0.04	0.16	0.05	n/a
Range ($\delta^{18}\text{O}$ ‰)	0.05	0.50	0.20	n/a
Number of samples	2	17	30	1

5

6

7 **Table 3: Comparison of observed and simulated (represented by the underlying pixel) SWE values at the plot-scale.**

Site	Date	Stage of snowmelt season	SWE [mm]		Difference between observed and simulated SWE [%]
			Observed	Simulated	
S1	2014-04-23	Early melt	141	151	7
N1	2014-04-23	Early melt	351	356	1
Wind	2014-04-24	Early melt	201	229	14
S1	2014-04-25	Early melt	113	78	-31
N1	2014-04-25	Early melt	270	293	9
N2	2014-06-07	Peak melt	594	477	-20
N2	2014-06-08	Peak melt	568	435	-23
N2	2014-06-09	Peak melt	537	390	-27
Mean deviation between observed and simulated SWE					13

8

9

10 **Table 4: Isotopic characterization of the event water component by the applied weighting techniques**

	Event water isotopic composition ($\delta^{18}\text{O}$ ‰)			
	23/04	24/04	07/06	08/06
VWS	-17.9	-18.2	-17.5	-17.5



VWO	-18.3	-18.6	-17.4	-17.5
VWE	-18.1	-18.3	-17.5	-17.5
NORTH	-18.6	-18.8	-17.9	-17.9
SOUTH	-17.6	-17.9	-17.1	-17.1

1

2

3 **Table 5: Discharge quantities of the Rofenache for the early and peak melt event at the outlet of the basin.**

	Event	
	Early Melt	Peak Melt
Date	23/04 – 25/04	07/06 – 09/06
Mean discharge	1.5 m ³ s ⁻¹	11.5 m ³ s ⁻¹
Peak discharge	1.9 m ³ s ⁻¹	17.4 m ³ s ⁻¹
Volume runoff	3.3 mm	20.7 mm
Mean event water fraction	35±3 %	75±14 %
Peak event water fraction	44 %	78 %

4

5

6 **Table 6: Event water contribution to streamflow estimated with different weighting techniques. The error indicates**
7 **the variability (standard deviation) and the brackets depict the range.**

	Event water contribution (%)				
	VWS	VWO	VWE	NORTH	SOUTH
Early melt event	35±6 (25-44)	30±4 (22-35)	33±5 (24-39)	28±3 (21-31)	40±9 (28-55)
Peak melt event	75±2 (70-78)	78±3 (71-82)	76±2 (70-78)	66±2 (60-67)	90±3 (84-94)

8